PB 197 100

REMOTE SENSOR APPLICATION STUDIES PROGRESS REPORT, JULY 1, 1968 TO JUNE 30, 1969. REMOTE SENSING RECONNAISSANCE, MILL CREEK AREA, ARBUCKLE MOUNTAINS, OKLAHOMA

L. C. Rowan, et al

Geological Survey
Washington, D. C.

1970

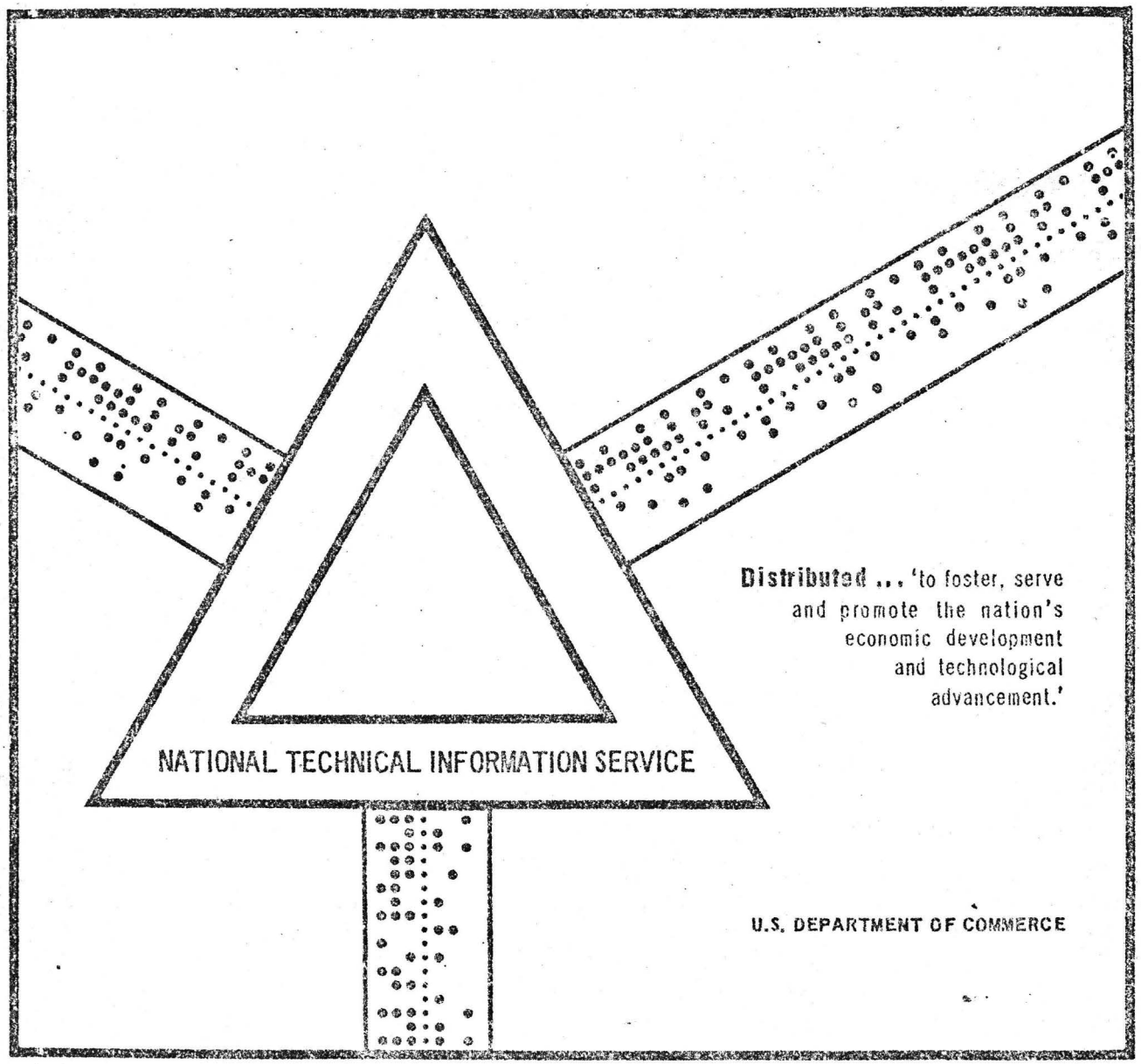

UNITED STATES

DEPARTMENT OF THE INTERIOR

GEOLOGICAL SURVEY

REMOTE SENSOR APPLICATION STUDIES PROGRESS REPORT, JULY 1, 1968 to JUNE 30, 1969

REMOTE SENSING RECONNAISSANCE, MILL CREEK AREA, ARBUCKLE MOUNTAINS, OKLAHOMA

by

L. C. Rowan, T. W. Offield, Kenneth Watson,

P. J. Cannon, and R. D. Watson

Prepared by the U.S. Geological Survey for the

National Aeronautics and Space Administration (NASA)

(Work performed under NASA Task 160-75-01-43-10)

1970

This report is preliminary and has not been edited or reviewed for conformity with U.S. Geological Survey standards and nomenclature.

CONTENTS

ILLUSTRATIONS

Remote Sensing Reconnaissance, Mill Creek Area, Arbuckle Mountains, Oklahoma

By L. C. Rowan, T. W. Offield, Kenneth Watson
P. J. Cannon, and R. D. Watson
U.S. Geological Survey
Denver, Colorado

INTRODUCTION

As part of the U.S. Geological Survey's Remote Sensor Application Studies program, infrared images and several kinds of photographs were obtained on reconnaissance flights over two areas in the Arbuckle Mountains near Mill Creek, Oklahoma. These data were used in a preliminary investigation (1) to determine the diagnostic reflection and emission characteristics of various rock types, and (2) to evaluate the perturbing influence of atmospheric conditions, surface coatings, rock texture, and topography on the observed reflected and emitted energy in the thermal infrared (8-14μ) part of the spectrum.

The areas flown are called here the Tishomingo anticline area (locally known as Rock Prairie) and the South Flank (of the Arbuckle anticline) area (fig. 1). They cover about 80 and 75 square miles, respectively, and are separated by about 20 miles. These test areas provide good exposure of several mineralogically simple rock types in different structural and topographic settings. Preliminary analysis of the reconnaissance data has yielded considerable insight into the numerous factors affecting the reflection and emission characteristics of rocks.

The data were acquired on December 19-20, 1968, by instruments aboard the NASA Earth Resources Program Convair 240A aircraft. The flights were part of NASA Mission 84, under NASA task 160-75-01-43-10.

GEOLOGY

The areas studied are located on the south flank of the Arbuckle Mountains uplift in south-central Oklahoma. Rocks of interest in these areas range in age from Precambrian to Pennsylvanian; they were folded and faulted when the uplift formed in Pennsylvanian time. The generalized geology of the areas is shown in figures 2 and 3.

The two areas are in different physiographic and structural provinces separated by the Washita River. The Tishomingo anticline area, east of the river, consists of gently rolling hills where the relative relief is approximately 100 feet and is underlain by gently dipping beds. It was selected because differences in rock type dominate the infrared images, whereas the effects of topography and structure are subordinate. The South Flank area, west of the river, is underlain by carbonate rocks and shales, and the topographic relief is about 200 feet. The difference in topography is due mainly to differential weathering of the shales and carbonates. Topographic effects in the South Flank area would dominate the imagery at the expense of differences in rock type.

Rock units of principal interest are the abundant, relatively pure dolomites, limestones, and sandstones in the Cambrian-Ordovician section, and Precambrian biotite granite exposed in the core of the Tishomingo anticline. Other rock types in the areas include shale, chert, arkose, granitic gneiss and quartz conglomerates, and transitional types such as dolomitic limestone, argillaceous limestone, and sandy dolomite, but these are not considered in the present study. In the South Flank area, the topographic effects of interest reflect differences in strata ranging in age from Cambrian to Pennsylvanian.

Cambrian-Ordovician stratigraphic relations in the southern Arbuckle Mountains are complex (Ham, 1955), and only those relations pertinent to the analysis of the remote sensing data will be mentioned here. Figure 4 shows the Precambrian-Cambrian-Ordovician geologic section of the Tishomingo anticline area. Some of the stratigraphic units are difficult to recognize not only on photographs and images but in the field as well, because the boundaries were defined mainly on faunal data. It is possible, however, to distinguish certain rock types in the photographs and images, and where these rock types characterize geologic map units, stratigraphic determinations can be made through remote sensing techniques.

Cambrian dolomites comprise a thick sequence in the Tishomingo anticline area (fig. 4). The Royer dolomite, which forms the largest part of the sequence, shows only minor variations in its outcrop characteristics; it is dark to very dark-gray and has highly pitted ledges or castellated pedestals. The Honey Creek Formation is composed of sandy dolomite and commonly occurs as boulders or rounded pedestals; the Butterly is composed of dolomitic limestone and is somewhat more thinly bedded and lighter in color than the purer dolomites. The dolomites of the Fort Sill Formation are similar in color and texture to those of the Royer, but show a facies change to limestone.

Limestone is abundant in the Middle- and Upper-Ordovician units of the South Flank area, but only the Fort Sill and the McKenzie Hill formations offer good exposures of limestone in the Tishomingo anticline area (fig. 4). The limestones of the Tishomingo anticline area are commonly relatively impure, with argillaceous material, chert, and dolomite comprising the main impurities; in places, thin sandstone beds occur. Most of the limestones are light gray to light bluish-gray and form rubbly, platy outcrops; however, a massive, moderatley dark-gray limestone marks the top of the Bromide Formation, and some dark-gray limestone is present in the McKenzie Hill Formation.

Both dolomites and limestones form flat to gently rolling prairies bearing a sparse growth of grass in the Tishomingo anticline area, but in the South Flank area the steeply dipping beds of limestone form hogbacks between valleys underlain by shale.

In contrast to the limestones and dolomites, the sandstones of the Reagan and Simpson Group and the Tishomingo Granite are tree covered, and 50 to 75 percent of thier outcrop surfaces are coated by lichen and moss. Prominent lineaments and somewhat greater topographic expression distinguish granite outcrops from sandstone outcrops.

The two areas cover parts of major anticlines which trend west-northwest and dominate the structural pattern of the region. In the Tishomingo anticline area poorly developed fracture systems, which show well only on infrared images, are parallel to the major anticline axis and to cross faults noted on the geologic map (fig. 2). In the South Flank area, fracture systems are well developed parallel and perpendicular to the axis of the Arbuckle anticline and are associated with cross folds and cross faults which distort the south flank of the anticline.

IMAGE ANALYSIS

Data obtained

Data acquired over the test areas during Mission 84 included Ektachrome and Ektachrome infrared photographs, and Reconofax IV infrared images. Black-and-white photographs in nine spectral bands obtained for part of the Tishomingo anticline area have not been analyzed fully. Preliminary analysis suggests that they may be useful for recognizing carbonate rocks of different compositions. Microwave single-scan data were obtained but have not yet been processed for study. Information concerning the photographs and images analyzed for this report is given in table 1.

Table 1. Flight and format parameters for photographs and images of the Mill Creek, Okla., test site.

Type of Data	Time of Acquisition (CST)	Number of Frames	Format	Scale	Identification Resolution (feet)	Total Areal Coverage (sq. mi.)
Ektachrome Photographs (0.4-0.7μ)	2:30 p.m.	94	9 x 9 inch	1:11,700	2	115
Ektachrome infrared Photographs (0.5-0.9μ)	2:30 p.m.	95	9 x 9 inch	1:11,700	2	115
Reconofax IV Images (8-14μ)	11:00 a.m.	3 strips	70-mm strips	1:45,000 to 1:55,000	25-35	228
	2:00 p.m.	3 strips				228
	6:00 a.m.	4 strips				223

Near-ground air temperature and relative humidity were measured and recorded continuously by a hygrothermograph during a 72-hour period starting at noon on December 17, 1968. The measurements provide a basis for modeling atmospheric perturbations that may affect the diurnal cooling rate. Other ground measurements included quartz-sand and lake-water temperatures and were useful in providing quantitive bounds for the theoretical cooling curves used in data interpretation. Later flights will use calibrated sensors and magnetic tape recording for optimum data fidelity; an extensive program of ground-temperature measurements will be essential for maximum utilization in geologic studies.

Ektachrome and Ektachrome infrared photographs

Ektachrome and Ektachrome infrared photographs were obtained for the Tishomingo anticline and South Flank areas in order to assess their value for determining the visible and near-infrared reflectivity of the rock and soil and the influence of surface coatings, vegetative cover, texture, and topography in masking or enhancing those parts of the reflection spectrum that might be characteristic of rock type composition. The Ektachrome film, Kodak No. 8442, is mainly sensitive to the visible part of the spectrum (0.4-0.7 microns), whereas Ektachrome infrared film, Kodak No. 8443, is sensitive to green, red, and near-infrared radiation (0.5-0.9 microns). Thus, "true" colors are recorded on the Ektachrome and "false" colors are presented on the Ektachrome infrared photographs; on the latter photographs, infrared radiation is recorded as red, red as green and green as blue.

The value of Ektachrome infrared photographs in the study of vegetation has been illustrated by Colwell (1968) and by Carneggie and Reppert (1969). Enhancement of vegetative differences results from the relatively high reflectance of vegetation in the extreme red and infrared parts of the e-m spectrum (0.7-0.9 microns). Because vegetation commonly develops along structural features, in response to soil and moisture concentrations, Ektachrome infrared photographs aid in the location and delineation of these features.

In Mill Creek test areas both the Ektachrome and Ektachrome infrared photographs have high spatial resolution (table 1) and fine color contrast. Subtle color differences are readily detected on the Ektachrome photographs, and therefore the major rock types are usually distinguishable. Differences in the type and distribution of vegetation are primarily dependent upon the climatic conditions and chemical and physical characteristics of the soils present. The climate in south-central Oklahoma is temperate and the soils are mainly residual clay loams with varying amounts of sand and weathered rock fragments. In some places, the residual soil types, and therefore the bedrock variations, are determinable on the Ektachrome infrared photographs due to changes in the vegetation. Vegetation concentrated along fractures, joint, and bedding planes is also enhanced on the infrared photographs and in many places the distinction between outcrop and residual soil was best made on these photographs. Ektachrome infrared photographs taken during the height of growing season (mid-June through July) might be even more diagnostic than those acquired during Mission 84.

Comparison of black-and-white photographs with photographs from the two strips of Ektachrome and Ektachrome infrared covering parts of this study area showed that the Ektachrome photographs are especially useful for determining the qualitative response of the major rock types to radiation in the visible part of the e-m spectrum. Of particular interest for analysis of the infrared images are estimates of the total energy absorbed by the limestones, dolomites, the granite, and sandstones. Typically, the limestones are very bright and light bluish gray, whereas the pure dolomites are consistently very dark gray; in a few places, nearly white, rubbly, but relatively continuous narrow bands of impure dolomites are even brighter than the limestones. It is therefore to be expected that the darker and rough-textured dolomites absorbed more energy than the lighter, more reflective limestones. Differentiation of the sandstones and granite is a more difficult problem due to the moss and lichen cover and density of foliage. Both the Tishomingo granite and the arkosic Reagan Sandstone show through the dense foliage as mottled, conspicuous outcrops, but the granite is distinctly more blocky and more massive than the sandstone. These and other parameters are discussed in more detail in a later section. In general, analysis of the color photographs provides essential information for interpretation of the infrared images and improves the ability to discriminate rock types.

Reconofax IV infrared imagery

Infrared (8-14 microns) images were obtained at three different times (table 1) in the Tishomingo anticline and South Flank area in order to relate surface temperatures to the diurnal heating cycle.

The imaging system used, Reconofax IV (HRB Singer RX-IV), has an instantaneous field of view of 3 milliradians and an angular scanning width of 120° perpendicular to the flight path. The flight altitude was 5,000 feet above mean ground elevation, and the mean ground identification resolution is estimated to be 30 feet near the nadir. The thermal resolution of the Reconofax IV system is 0.25°C.

The infrared images have good contrast and an optimum identification resolution of about 30 feet. The principal difficulties in analyzing the images arise from calibration problems and image geometry distortions. External calibration of the images is complicated both by an apparent limited dynamic range in the film-recorded images and by lack of internal drift correction. For example, the temperatures of the north and south lakes at the Mill Creek sand quarry as obtained with the Barnes radiometer show 4° to 5° differences between the 11:00 a.m. overflight on December 19 and the 6:00 a.m. overflight on December 20. Yet no apparent difference in the radiative flux from the two lakes is detectable on the images. In addition, the consolidated quartz sands near the two lakes demonstrate even greater temperature contrasts which cannot be detected on the images. This lack of sensitivity due to limited dynamic range can be rectified by recording future data on magnetic tape and at a variety of gain settings to optimize the full range of small variations in infrared intensity. The geometric distortions on the edges of the images reduce the useful width of the image that can be analyzed; this problem can be alleviated by obtaining flights with large side lap.

Tishomingo anticline area

The part of the Tishomingo anticline area selected for detailed analysis lies south and southwest of the town of Mill Creek (figs. 3 and 5). Although the stratigraphic sequence detailed in fig. 4 can be fully recognized in the field, some of the formations are, as previously mentioned, difficult to discriminate from the overlying Fort Sill Formation, and the Butterly Dolomite is in transitional contact with limestones of the McKenzie Hill Formation above and the Royer Dolomite below.

Shown in figure 5 are the major rock-type variations in part of the Tishomingo anticline area; from east to west the sequence is from oldest to youngest rocks as shown in figure 4. The units most easily recognized on the black-and-white photomosaic (fig. 5) are the Tishomingo granite, the Reagan Sandstone, the alternating dolomites and limestones of the Honey Creek and Fort Sill Formations, the Royer and Butterly Dolomites, and limestones of the Butterly and the McKenzie Hill. Also shown on the photomosaic are limestones of the Upper Arbuckle Group, but these rocks were not imaged by the Reconofax IV system. Equivalent rocks are covered by infrared data of the South Flank area but have not yet been examined in the field for comparative purposes. It must be emphasized that although identification of the granite is not difficult on the photomosaic, differentiation of the limestones and dolomite is either very difficult or impossible even after considerable familiarity with the area has been attained.

Of the three times during which the infrared images were obtained, the predawn (6:00 a.m.) images appear to be most useful in distinguishing rock types, particularly limestone and dolomite. Shown in figure 6 are the two daytime and the predawn infrared images of the south-southwestern

part of the Tishomingo. Most striking is the predawn image (fig. 6a) which shows an anomalously bright (warm) area near the center of the image. The rocks of this area are mainly dolomites and biotite granite, whereas the adjacent, relatively dark area (cool) is underlain chiefly by limestones in the Fort Sill and McKenzie Hill Formations. Considerable detail can be discerned in these areas. For example, sedimentary layering in the limestone is conspicuous as alternating light and dark tones; it is less obvious in the dolomite except where dolomite and limestone alternate in the Fort Sill Formation. At point A in figure 6a , dolomite changes to limestone through a facies transition in the Fort Sill Formation, an observation of considerable geologic significance. This transition is clearly defined on the image by the thermal contrast of the dolomite and the limestone along strike. This type of warm-cool contrast should not be confused with other prominent dark areas which are stream channels, particularly in the dolomites, and in areas of dense foliage, such as the areas underlain by the Regan Sandstone and the Tishomingo Granite. This distinction between limestone and dolomite by radiometric character is similar to the distinction between sandstones and siltstones noted by Sabins (1967) and of various other rock types by Friedman (1968). Stratigraphic units have been distinguished elsewhere by radiometric differences, but these differences are generally ascribed to vegetative cover on different rock types rather than to inherent rock properties (e.g., Lattman, 1963).

In order to evaluate the radiometric differences between the limestones and dolomites, film-density measurements of the nighttime image were made

using a Joyce-Loebl recording microdensitometer. Shown in figure 7 is one of the density profiles prepared (line F-F, fig. 6a). Although there is considerable variation in film density within the limestone and the dolomite areas, it is clear that the dolomites have characteristically (up to 15%) lower film density and therefore higher total emission. Notable features on the profile are a small pond and the high frequency and large amplitude of film-density variations in areas of relatively dense foliage and small, cool stream channels. Although the granite is not included in this particular density profile, the profile also shows a film density approximately equivalent to the dolomites but with higher amplitude film-density variations indicating larger total emission contrast.

Within the limestone and the dolomite sequences are relatively dark (cool) areas on the predawn image (fig. 6a). Most of these correspond to drainage channels in a dendritic pattern or to areas of dense foliage (point B, fig. 6a). In the southern central part of this image, however, are several prominent intersecting dark bands. Three of these, indicated by C, D, and E on figure 6a , are strikingly linear and were examined in the field, on the topographic map (fig. 8), and on all available photographs. These areas are saturated with ground water and are fracture or fault zones; significantly, they are not all topographically lower than the surrounding terrain, and are not readily detectable on conventional photographs. For example, in figure 3 , the northwest-trending feature is a topographic depression, perhaps a graben, northwest of C, but to the southeast of this point the linear feature transects topographic highs. Of the two north-trending fracture zones (points D and E,

fig. 6a), only the one with the two ponds (E) occupies a topographic low for a significant distance along its trend; the other band transects the east side of a rounded hill (fig. 8) for most of its extent.

Because water saturates these fracture zones, the most adequate explanation for the relatively low emission appears to be that these areas have cooled by evaporation. This explanation may also be sufficient to explain the low emission in the drainage channels. Settling of cold air in the topographic lows will also contribute to heat loss in these areas.

The daytime infrared images of the Tishomingo anticline area show, in some places, excellent definition of sedimentary layering and fracture zones (fig. 6b and 6c). On the 11:00 a.m. image shown in figure 6b , sedimentary layering, which generally trends north to northwest, is conspicuous on sunward (southeast) slopes. Although fracture and joint traces are not well displayed on the 11:00 a.m. image, traces trending west-northwest extend from the granite near the southeast border of the image into the Cambrian sandstone and carbonates and into the northern part of the area. Northeast-trending joint and fracture traces are detectable in a few areas near the center of the image. Unlike the areas of prominent bedding, these features appear to be essentially independent of local topography.

The infrared image of the Tishomingo anticline area obtained at approximately 2:00 p.m. (fig. 6c) shows only a few areas of bedding (in which the thermal contrast probably reflects the total integrated effect of insolation as the sun azimuth changed through the morning).

Structural information shown is mainly restricted to fracture traces, trending east-northeast, which are prominent in the southern part of the area shown in figure 6c. The occurrence of these traces does not appear to be significantly affected by the topography inasmuch as topographic highs and lows with variable orientations to the sun are transected. These factures are not as apparent on any of the available photographs as they are in the infrared image.

South Flank area: Structural and stratigraphic information displayed in the infrared images of the South Flank area stems mainly from the excellent definition of bedding in the daytime images. The 11:00 a.m. image (fig. 9a) shows a remarkable "grain" of bedding by density contrasts. Presumably the bright stripes are groups of beds, as single beds generally are smaller than the ground resolution limit. Formation contacts, however, are poorly defined. In the 2:00 p.m. image (fig. 9b), the "grain" of bedding is not so conspicuous and small-scale bright-dark contrast is less than at 11:00 a.m. However, several formations are readily distinguishable and their contacts fairly sharply defined. The 6:00 a.m. image (fig. 9c) shows many conspicuous groups of beds as brighter (warmer) than their surroundings. Included in the brighter areas are diverse lithologies such as white-weathering, fine- grained, impure dolomite and dark-gray, coarse-grained, crystalline limestone. Formation contacts are not well defined. The area marked "A" on figures 9 a, b, and c provides a comparison of stratigraphic information obtained at the different flight times.

Structural information in the infrared images is derived from such an excellent display of bedding that faults and folds are clearly evident (see Sabins, 1969, for a comparable example), and from the display of lineaments. Many of the latter cannot be seen in color or black-and-white photographs. The lineaments (areas of prominent lineaments indicated by arrows on the three images) are of particular interest because some of them are visible only on infrared images and because they are important to interpretation of the overall structure of the area. Only northwest-trending lineaments are visible in the 11:00 a.m. images; only those trending northeast aré seen at 2:00 p.m.; and only rare ENE lineaments show at 6:00 a.m. The lineaments appear warmer than adjacent ground. Some can be seen on photographs as grassy low zones along fractures, but most cannot be recognized. Field observation shows the three major directions of lineaments to coincide with joint sets, but the extent of single lineaments and their overall abundance is nearly impossible to determine except in infrared images.

Another interesting structure best defined in the infrared images is a fault zone indicated on the 2:00 p.m. and 6:00 a.m. images. It is obscured by minor topographic and thermal effects at 11:00 a.m. Part of the zone can be traced on photographs because it shows as a grassy zone between outcrop ridges. On the infrared images, however, and particularly at 6:00 a.m., the exact width of the broken zone along the fault is clear. The width varies considerably in short distances, and is defined by a strip cooler than adjacent ground. Field examination shows that this strip is not consistently a topographic low, and we conclude that the coolness is related to ground water

concentrated in the zone of broken rock. This has interesting implications with respect to locating and defining such zones elsewhere for engineering, ground water, and mining purposes.

THEORETICAL CONSIDERATIONS AND INTERPRETATION

Parameters effecting infrared images

The emitted thermal flux that is sensed by the infrared detector of the imaging system is a function of three major classes of parameters: (1) rock or surficial soil parameters (albedo, thermal inertia, emissivity); (2) insolation parameters (sun's declination, latitude of site, local time, and local topography); and (3) atmospheric parameters (transmission, nighttime sky radiation, and evaporative cooling).

Because insolation provides the driving function to heat both ground and atmosphere, the ground surface temperature during the daytime is dominated by the insolation parameters and by the surface albedo. (The absorbed flux is the product of the local insolation, the cosine of the local zenith angle, and the co-albedo.) During the nighttime, the effects of the atmospheric parameters and the rock thermal inertia have a significant effect on the surface temperature and in general their roles are more pronounced just before sunrise when insolation effects are least important. In general, then, it is expected that daytime infrared images should be most responsive to variations in local topography and co-albedo, and nighttime infrared images to variations in atmospheric effects and thermal inertia. Variations solely in emissivity of natural surfaces produce a proportionate change in the emitted flux. Exposed rocks are less efficient radiators than soils because, within the precision of imaging systems, all soils behave approximately as black bodies, independent of their composition.

Daytime infrared images

The daytime images of the Tishomingo anticline area show that bedding detail is enhanced on sunward topographic slopes, and that lineament sets are preferentially displayed in either the morning or afternoon, depending on the direction in which they trend. In the South Flank area, where hogbacks formed by dipping formations are numerous, the marked contrast between conspicuous formation delineation in the afternoon image and pronounced "grain" of smaller scale bedding in the morning image is clearly a topographic effect related to time of day. Preferential display of lineaments at the two times is similar to that in the Tishomingo anticline area.

In order to analyze the directional character of insolation parameters that contribute to the observed effects, a mathematical model of the diurnal temperature variation of an inclined planar element was constructed to determine the strike azimuth at which the computed temperature changes most rapidly with slope angle (Watson, 1970, p. 24). This direction (thermal strike) should provide an indicator of (1) optimum daily and seasonal times to enhance (or suppress) topographic lineaments, and (2) the insolation contribution to linear trends observed on daytime infrared images. In addition, the direction for most rapid change in insolation with slope angle (insolation strike) was also computed.

The results for the Mill Creek areas (latitude 34.5°, sun declination -23.3°) are presented in figure 10 (thermal and insolation strike versus time), with arrows indicating the approximate times at which the images were obtained. The model predicts thermally enhanced strike direction

of N. 25° E. for the morning flight and N. 80° E. for the afternoon flight. The calculations also predict that the insolation strike (best observed in visible and near-infrared photographs) should enhance a morning direction of N. 79° E. and an afternoon direction of N. 70° W. Presumably both sets of directions should be present to some degree on the infrared imagery since the former (thermal strike) should reflect moderate slopes and the latter (insolation strike) should reflect steeper slopes which cast shadows. Lineaments are not primarily topographic features and apparently do not owe their prominence on the images to these factors, but the "grain" of bedding and formations is a topographic expression and is enhanced as the model predicts in many places. Images of the Tishomingo anticline area (southern edge, fig. 6) show the afternoon enhancement of topographically conspicuous formations parallel to the maximum insolation strike. The infrared images of the South Flank area (fig. 9) illustrate the prominence of features parallel to the afternoon thermal strike and, possibly to a lesser degree, parallel to the morning insolation strike.

The difference in stratigraphic information contained in the two daytime images of the South Flank area appears to result from topographic scale effects. The morning image shows bedding emphasized by small-scale but conspicuous bright-dark (warm-cool) contrast due to the preferential heating of the sunward sides of ridges. The afternoon image shows a significant reduction in this thermal contrast inasmuch as both sides of the bedding ridges have received illumination from the sun which tends to equalize their temperatures. But the opposite faces of hogbacks, which are larger scale features with steeper slopes, retain the thermal contrast

because shadowing and hence insolation differences are still present. In summary then, average slope differences at the two topographic scales result in an enhancement of bedding detail in the morning image and of whole formations which form the hogback-valley system in the afternoon image.

Nighttime infrared images

Because the nighttime images showed strong thermal contrast between limestone (cool) and dolomite (warm), an attempt was made to interpret the observations in terms of a model which seemed consistent with the field observations and which could be tested by later flight measurements. A simplified model of the rock parameters for the limestone and dolomite was used to compute theoretical cooling curves (Watson, 1970, p. 4). The results (fig. 11) illustrates the mutual enhancement from the lower albedo (due to weathering) and higher thermal inertia of dolomite (a compositional property) in raising its nighttime temperature with respect to that of limestone. During the daytime the two parameters work against each other; the higher thermal inertia tends to reduce the dolomite temperature and the lower albedo tends to increase it. Hence, the daytime temperature differences between limestone and dolomite are less useful as a diagnostic tool. But at nighttime, maximum contrast should be expected between rock types that combine maximum differences in albedo and thermal inertia, provide that a lower albedo is paired with a higher thermal inertia. The converse, that is, that high (low) albedo paired with high (low) thermal inertia would provide maximum daytime contrast should also prove to be true, provided that the effects of the topography do not overwhelm the observed thermal distribution. A more rigorous test, now being

planned, will be made by repeatedly taking calibrated images to examine in greater detail the diurnal cooling curves of the rock types exposed in the Mill Creek site, especially for an intercomparison among the dolomites (low albedo, high thermal inertia), the limestones (high albedo, low thermal inertia), and the impure dolomites (high albedo, high thermal inertia).

Atmospheric parameters

The preceding discussion has omitted an evaluation of the influence of the atmospheric parameters in order to emphasize the types of geologic information that can be extracted from infrared images. It is clear that at nighttime the dominant features of the images are the thermal cold anomalies in topographic lows or water-saturated fracture zones. The most reasonable explanation is heat loss from the ground due to evaporation and the conduction of ground heat into cold, water-saturated mists which, being denser, collect in the topographic lows or do not disperse readily from above their water sources. Atmospheric effects (e.g., cloud cover) are also important in modulating the daytime insolation and, especially in wintertime when the insolation is minimal, in introducing various periodicities in the thermal cycle due to the passage of weather fronts. Thus as a more quantitative analysis of infrared data is undertaken, a more careful treatment of atmospheric effects, including ground and air measurements, will be required.

CONCLUSIONS

The infrared data obtained for this reconnaissance study contain significant stratigraphic and structural information. Perhaps the most important conclusion is that relatively pure limestones and dolomites of the test area can be differentiated in nighttime infrared images, and that facies changes between them can be detected along and across strike. Such discrimination of rock type is possible because of a combination of the inherently different albedo and thermal inertia properties of the limestones and dolomites, and doubtless the same distinction can be made in other areas with only a minimal amount of field observation as control.

Topography strongly influences the distribution and scale of stratigraphic information displayed in the infrared images. Sunward slopes display maximum bedding detail, and in some areas show very subtle lineaments preferentially either in morning or afternoon images, depending on the lineament trends. Bedding detail is enhanced in morning images of low-relief areas. Such detail is not prominent in afternoon images, which instead show contrasts at the scale of geologic formations wherever moderate-relief topography is controlled by the bedrock. This effect appears to be a direct function of the amount of sunlight received by sunward and shadowed slopes of different scale.

Fault or fracture zones are delineated on infrared images as thermal lows, apparently because of water saturation and concomitant evaporation. The images contain information on width and continuity of such zones that cannot be observed by reflected energy recorded in conventional photographs. Lineaments are well displayed on the infrared images, locally where no lineaments can be detected on ordinary photographs,

but their presence has been confirmed by field examination. The prominence of lineaments without noticeable topographic expression cannot be ascribed to insolation effects and does not appear to be simply related to ground water or vegetation concentration; this enhancement of linear features is not yet understood, but illustrates the use of the infrared images for structural geologic investigations.

REFERENCES

Carneggie, D. M., and Reppert, J. N., 1969, Large-scale 70-mm aerial color photos: Photogramm. Eng., v. 35, no. 3, p. 249-257.

Clark, S. P., Jr., ed., 1966, Handbook of physical constants (revised ed.): Geol. Soc. America, Mem. 97, 587 p.

Colwell, R. N., 1968, Remote sensing of natural resources: Sci. American v. 218, no. 1, p. 54-69.

Friedman, J. D., 1968, Thermal anomalies and geologic features of the Mono Lake area, California, as revealed by infrared imagery: U.S. Geol. Survey open file report.

Ham, W. E., 1949, Geology and dolomite resources, Mill Creek-Ravia area, Johnston County, Oklahoma: Oklahoma Geol. Survey Circular 26, 104 p.

Ham, W. E., 1950, Geology and petrology of the Arbuckle limestone in the southern Arbuckle Mountains, Oklahoma: Yale University, unpublished doctoral dissertation, 162 p.

Ham, W. E., 1955, Field conference on geology of the Arbuckle Mountain region, Oklahoma Geol. Survey Guidebook 3, 61 p.

Ham, W. E. McKinley, M. E., 1954, Geologic map and sections of the Arbuckle Mountains, Oklahoma: Oklahoma Geol. Survey.

Lattman, L. H., 1963, Geologic interpretation of airborne infrared imagery: Photogramm. Eng., v. 20, n. 1, p. 83-87.

Sabins, F. F., Jr., 1967, Infrared imagery and geologic aspects: Photogramm. Eng., v. 33, no. 7, p. 743-750.

Sabins, F. F., Jr., 1969, Thermal infrared imagery and its application to structural mapping in southern California: Geol. Soc. America Bull., v. 80, no. 3, p. 397-404.

Watson, Kenneth, 1970, Remote sensor application studies progress report, July 1, 1968 to June 30, 1969: Data analysis techniques; U.S. Dept. Commerce Natl. Tech. Inf. Service .

Figure 1. - Index map of Oklahoma showing Tishomingo anticline area (T) and South Flank area (SF) in the Arbuckle Mountains. Trends of major anticlines are also shown.

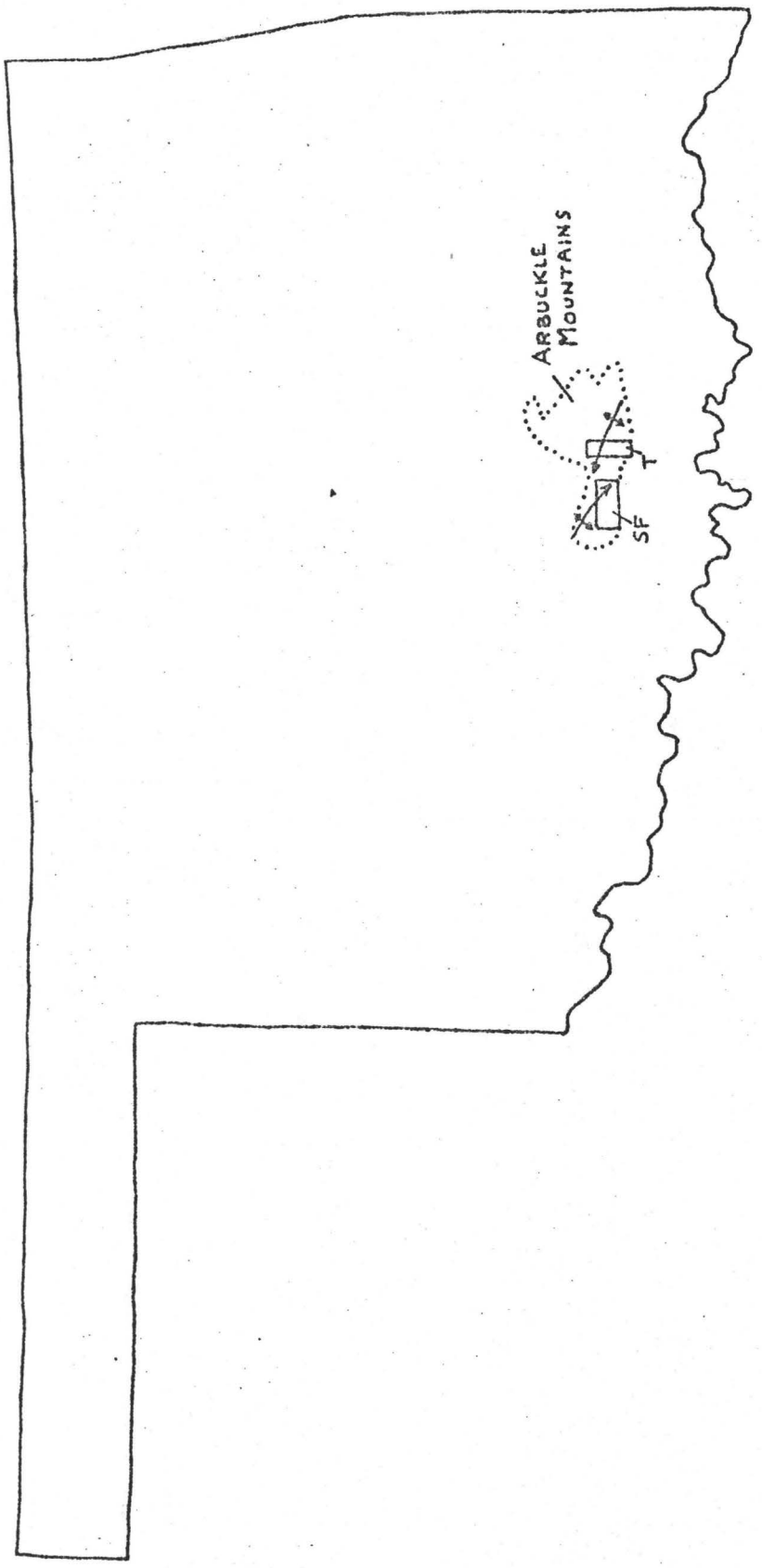
ARBUCKLE
MOUNTAINS
T
SF

Figure 2. - Geologic map of Tishomingo anticline area, Arbuckle Mountains, Oklahoma (from Ham, McKinley, and others, 1954). Reseau marks shown for matching with figures 5 and 6.

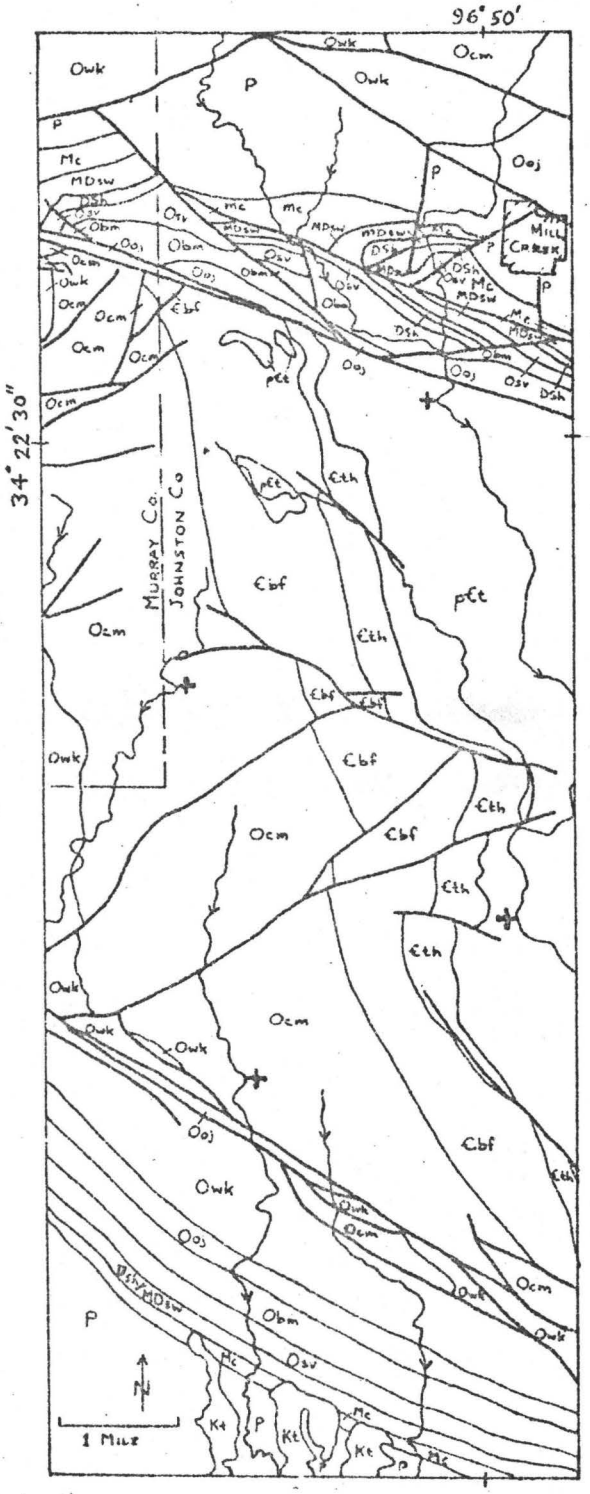
96° 50'
34° 22' 30"
MURRAY Co.
JOHNSTON Co
MILL CREEK
Owk
Ocm
P
Ooj
Mc
MDsw
DSh
Osv
Obm
Ocm
Cbf
pCt
Cth
Kt
1 MILE
N

Figure 3. - Geologic map of South Flank area, Arbuckle Mountains, Oklahoma (Ham, McKinley, and others, 1954). Reseau marks shown for matching with figure 9.

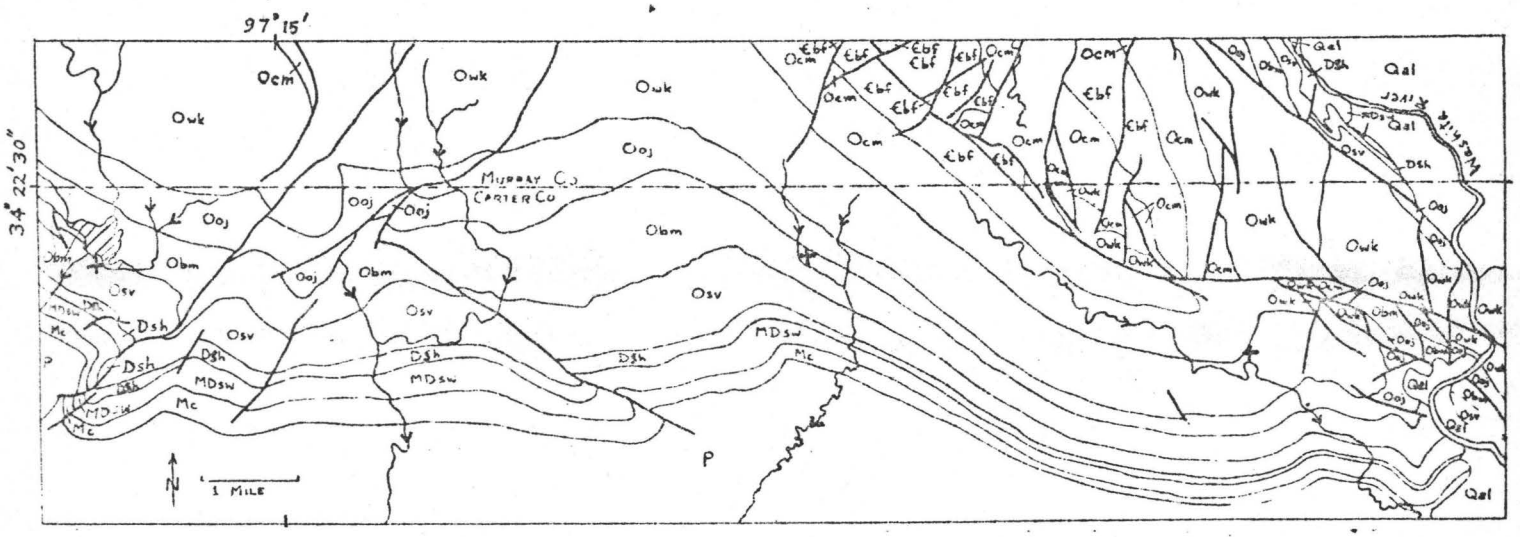
97°15'
34°22'30"
Ocm
Owk
Ooj
Obm
Osv
Dsh
MDsw
Mc
Ebf
Qal
MURRAY CO.
CARTER CO
P
N
1 MILE

EXPLANATION

FOR FIGURES 2 AND 3.

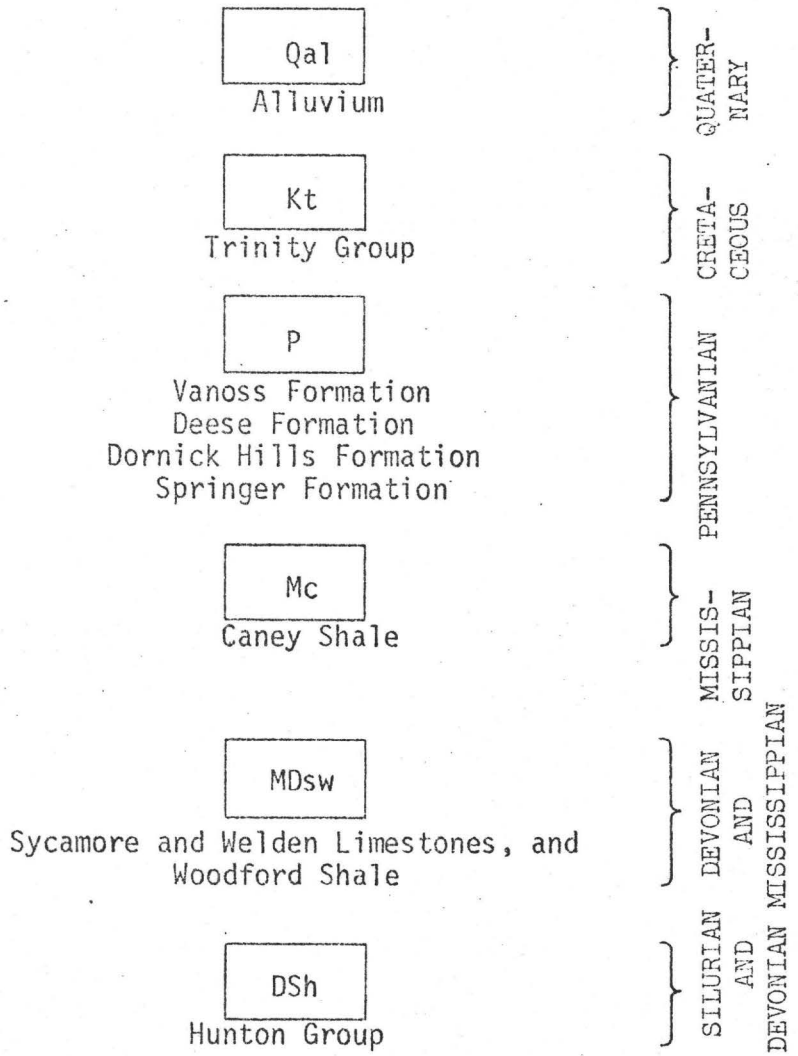

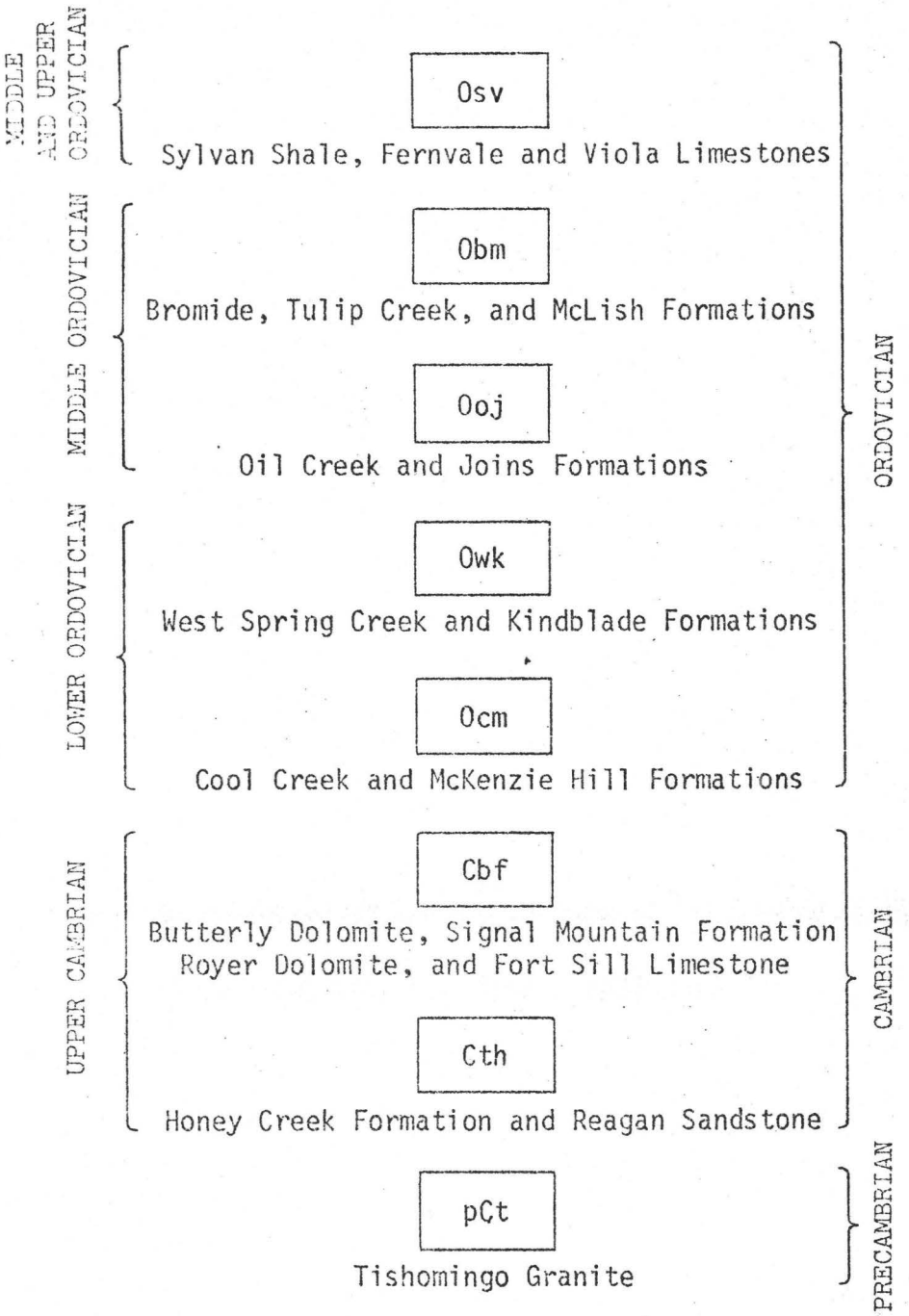
MIDDLE AND UPPER ORDOVICIAN
Osv
Sylvan Shale, Fernvale and Viola Limestones
MIDDLE ORDOVICIAN
Obm
Bromide, Tulip Creek, and McLish Formations
Ooj
Oil Creek and Joins Formations
LOWER ORDOVICIAN
Owk
West Spring Creek and Kindblade Formations
Ocm
Cool Creek and McKenzie Hill Formations
ORDOVICIAN
UPPER CAMBRIAN
Cbf
Butterly Dolomite, Signal Mountain Formation
Royer Dolomite, and Fort Sill Limestone
Cth
Honey Creek Formation and Reagan Sandstone
CAMBRIAN
pCt
Tishomingo Granite
PRECAMBRIAN
Contact
Fault

Figure 4. - Precambrian to Ordovician stratigraphic section, Tishomingo anticline area (modified from Ham, 1955).

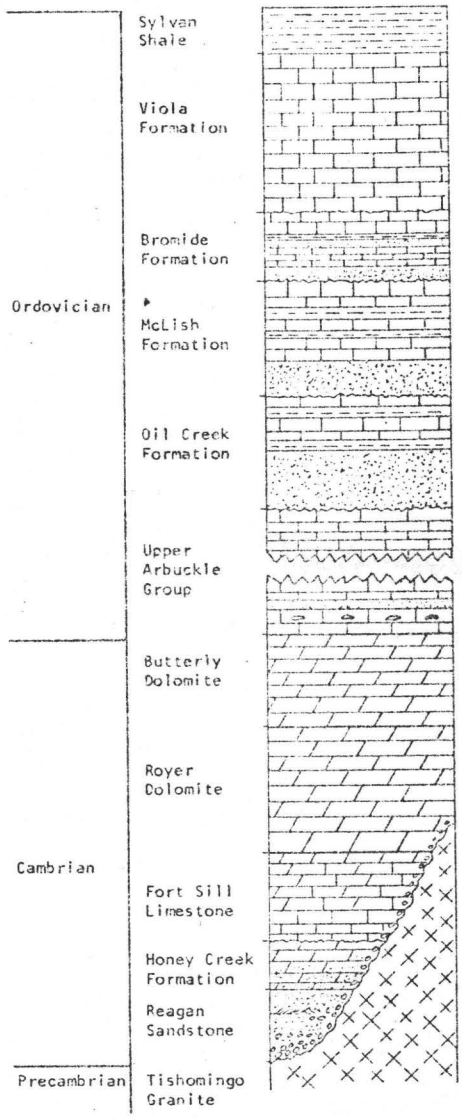
Sylvan Shale
Viola Formation
Bromide Formation
Ordovician
McLish Formation
Oil Creek Formation
Upper Arbuckle Group
Butterly Dolomite
Royer Dolomite
Cambrian
Fort Sill Limestone
Honey Creek Formation
Reagan Sandstone
Precambrian
Tishomingo Granite

Figure 5. - Photomosaic showing rock-type occurrence, Tishomingo anticline area (geology after Ham, 1949 and 1950: G, granite; S, sandstone; D, dolomite; L, limestone). Crosses shown for matching with figures 2 and 6. North at top of page.


SMITH
CREEK
T
G
L
D
L
L
D
D
D
L
D
D
G
L

Figure 6. - Infrared images of Tishomingo anticline area.

a) 6:00 a.m. (CST) image; point A--facies change from limestone to dolomite, B--drainage channel, C, D, E--fracture or fault zones, F-F'--line of isodensitracing profile shown in Figure 7 .

b) 11:00 a.m. (CST) image.

c) 2:00 p.m. (CST) image.

Reseau marks shown for matching with figures 2 and 5.

Scale approximately 1:90,000.

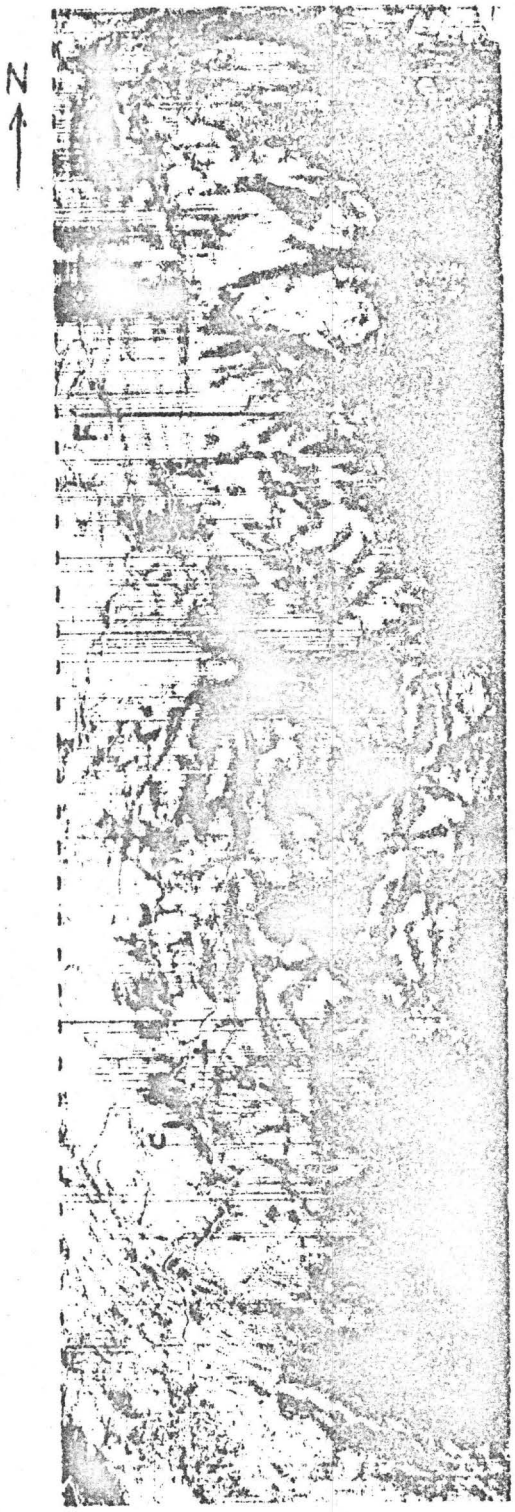
N

Figure 7. - Isodensitracing of limestone-dolomite area on nighttime infrared image, Tishomingo anticline area (line of profile shown on figure 6a).

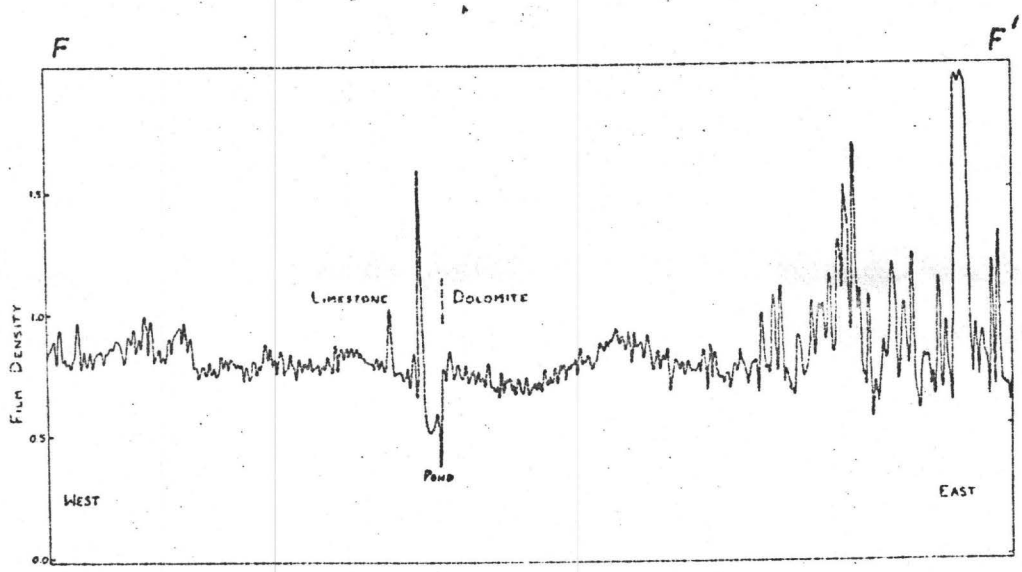
F
F'
FILM DENSITY
1.5
1.0
0.5
0.0
LIMESTONE
DOLOMITE
POND
WEST
EAST

Figure 8. - Topographic map showing cool linear zones shown at C, D, and E on Figure 6a.

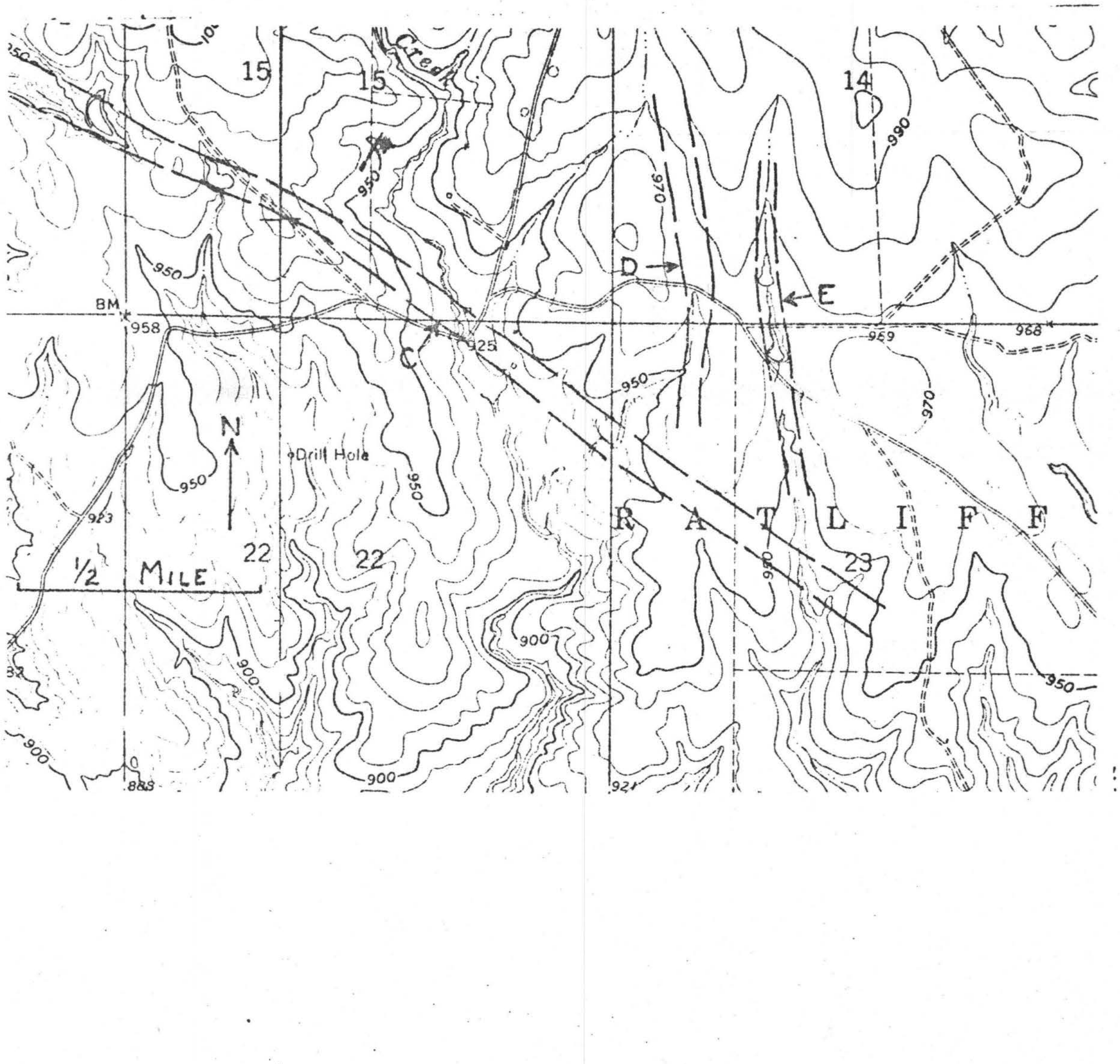
15
15
14
Creek
D
E
BM
958
925
959
968
950
970
990
900
923
N
Drill Hole
22
22
23
R A T L I F F
1/2 MILE

Figure 9. - Infrared images of the South Flank area.

a) 11:00 a.m. CST) image,

b) 2:00 p.m. (CST) image,

c) 6:00 a.m. (CST) image.

Area A demonstrates comparison of stratigraphic and structural information displayed at different flight times; areas of prominent lineaments marked by arrows. Reseau marks shown for matching with Figure 3 . Scale approximately 1:120,000.

Fig. 9a

Fig. 9b

Fig. 9c

Figure 10.- Strike computed from theoretical models for enhanced thermal contrast (T) and enhanced insolation contrast (I). The times for the morning and afternoon aircraft overflights that provide the infrared images are indicated. Local time is measured in hours from the time of local noon (0^{hr} local mean solar time = 12:28 p.m. CST).

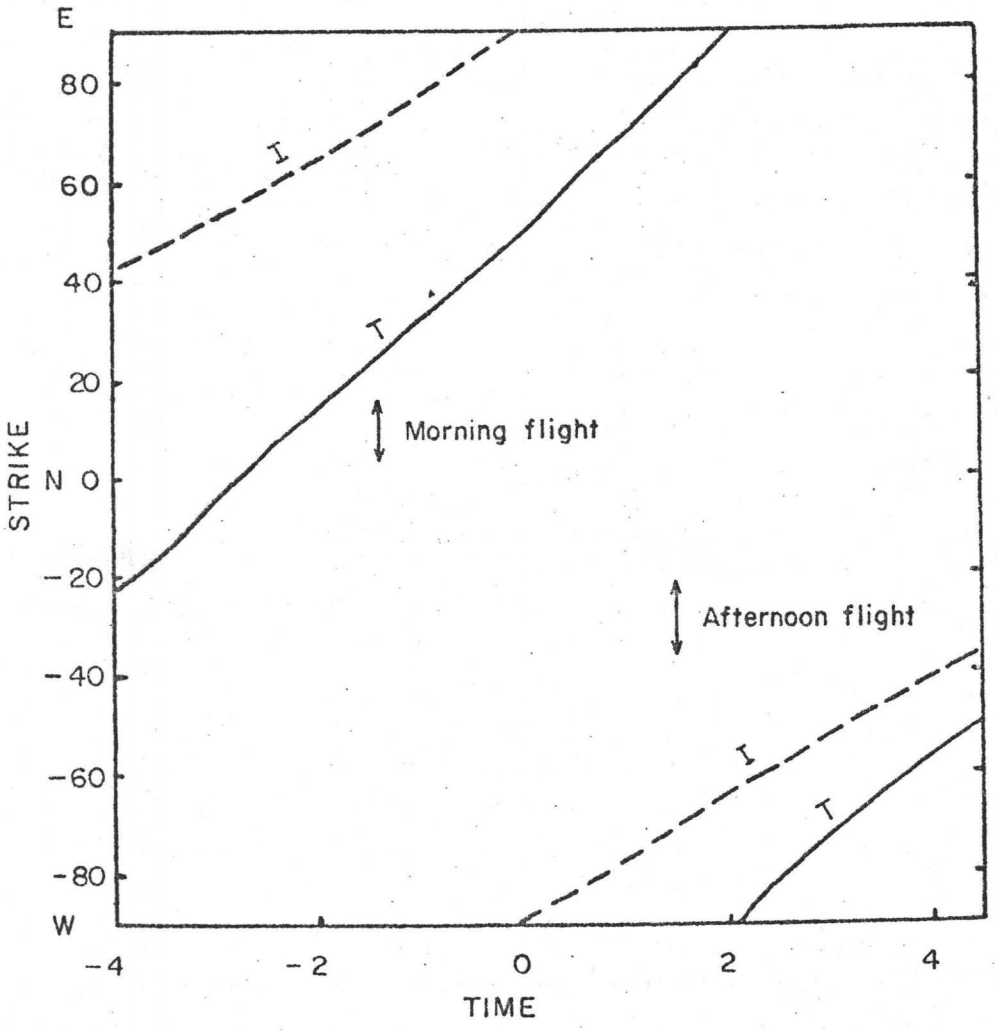
E
80
60
40
20
0
-20
-40
-60
-80
W
STRIKE
I
T
Morning flight
Afternoon flight
I
T
-4
-2
0
2
4
TIME

Figure 11. Theoretical cooling curves constructed using thermal inertias constructed from representative thermal property values in Clark (1966) and albedo values consistent with the observations that (1) the dolomite appeared darker than the limestone and (2) daytime temperature differences are not noticeable on the infrared images. (0^{hr} local mean solar time = 12:28 p.m. CST.)

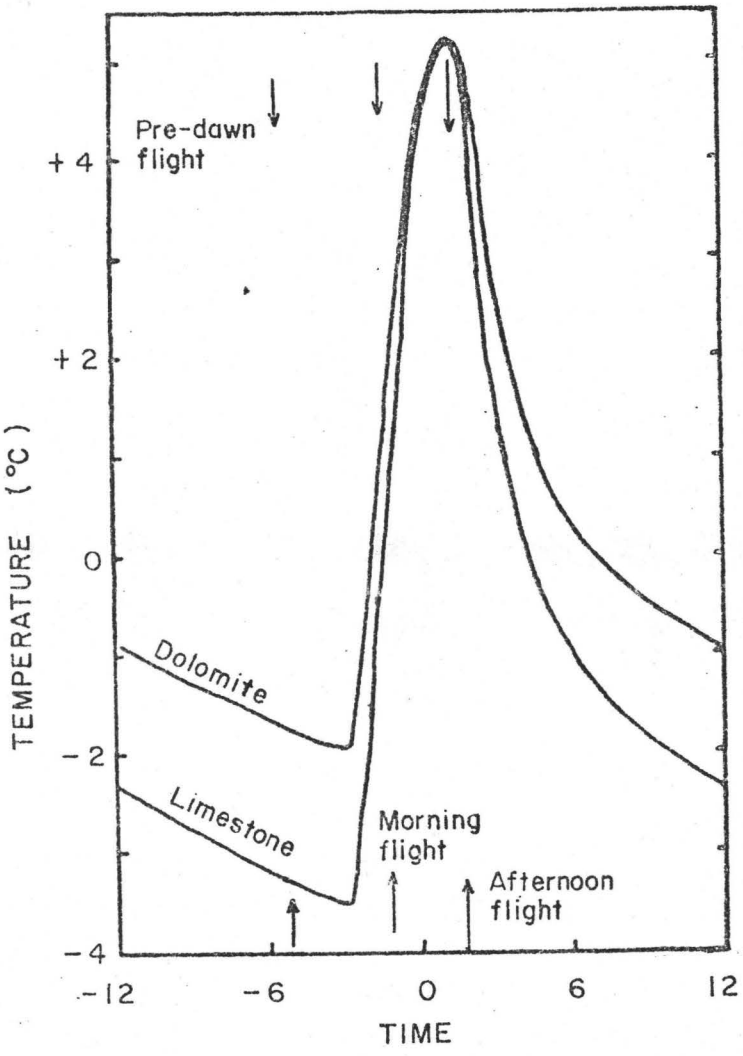
Pre-dawn
flight
+ 4
+ 2
0
- 2
- 4
TEMPERATURE (°C)
Dolomite
Limestone
Morning
flight
Afternoon
flight
-12
-6
0
6
12
TIME

STANDARD TITLE PAGE FOR TECHNICAL REPORTS | USGS-GD-71-008

4. Title and Subtitle
Remote sensor application studies progress report, July 1, 1968 to June 30, 1969: Remote sensing reconnaissance, Mill Creek area, Arbuckle Mountains, Oklahoma

5. Report Date
1970

6. Performing Organization Code

7. Author(s)
L. C. Rowan, T. W. Offield, K. Watson, P. J. Cannon, R. D. Watson

8. Performing Organization Rept. No.

9. Performing Organization Name and Address
U.S. Geological Survey
Washington, D. C. 20242

10. Project/Task/Work Unit No.

11. Contract/Grant No.

12. Sponsoring Agency Name and Address
National Aeronautics and Space Administration
Washington, D. C. 20546

13. Type of Report & Period Covered
Progress FY 1969

14. Sponsoring Agency Code

15. Supplementary Notes

16. Abstracts
Infrared data for the Mill Creek area in the Arbuckle Mountains of Oklahoma reveal significant stratigraphic and structural information. Relatively pure limestones and dolomites in this area can be differentiated in the nighttime infrared images, and the facies changes between them can be detected along and across the strike. This interpretation is possible because of the combination of the inherently different albedo and thermal inertia properties of the limestones and dolomites. Topographic alignment in relation to solar insolation strongly influence the scale and distribution of stratigraphic information which can be determined from the infrared images. Sunward slopes show maximum bedding detail and sometimes very subtle lineaments preferentially when imaged either in morning or afternoon. Fault and fractures are delineated in the infrared images as thermal lows, apparently due to evaporation of saturated zones. Lineaments, including some without noticeable topographic expression, are well displayed on the infrared imagery.

17. Key Words and Document Analysis. (a). Descriptors
Geology, infrared radiation, stratigraphy, geologic investigations

17b. Identifiers/Open-Ended Terms
Remote sensing

17c. COSATI Field/Group 08 G 20 F

18. Distribution Statement
Releasable to the public, available from NTIS, Springfield, Va. 22151

19. Security Class (This Report)
UNCLASSIFIED

21. No. of Pages
53

20. Security Class. (This Page)
UNCLASSIFIED

22. Price

FORM NBS-867(1-70)